

Transforming Palm Waste into Renewable Reductant: Torrefied Palm Kernel Shell as a Sustainable Reductant for Low-Carbon Ferronickel Production

Winny Wulandari^{1,*}, Akhmat Fauzan Saputra¹, Rama Haidar¹, and Taufiq Hidayat²

¹Department of Chemical Engineering, Faculty of Industrial Technology, Bandung Institute of Technology, Indonesia 40132

²Department of Metallurgical Engineering, Faculty of Mining and Petroleum Engineering, Bandung Institute of Technology, Indonesia 40132

Abstract. Indonesia, with the world's largest nickel ore reserves of approximately 55 million tons, plays a significant role in the global nickel supply chain. To support the national downstream strategy, efficient utilization of nickel ore, particularly through ferronickel production, is crucial. However, the conventional use of coal as a reductant poses the risk of increased carbon emissions in line with growing ferronickel demand, challenging Indonesia's Net Zero Emissions 2060 target. On the other hand, Indonesia also produces around 12.8 million tons of palm kernel shell (PKS) waste annually, which has potential as a low-carbon biomass reductant. Nevertheless, its low fixed carbon content limits its direct use in metallurgical processes. This research studied the torrefaction of PKS at 300 °C for 1 hour, which increased its fixed carbon content from 17.43% to 40.16%. The torrefied PKS was then used as a reductant for reducing saprolite nickel ore at a 1:4 w/w (reductant:ore) ratio, at temperatures of 500 °C, 700 °C, and 900 °C for 60 – 120 minutes. The reduced solids were characterized using XRD and SEM-EDS. Metallic phases were detected in samples reduced at 700 °C and 900 °C for 120 minutes, with iron (Fe) contents of 96.17% and 95.67%, respectively. These samples were subsequently smelted at 1373 °C, 1473 °C, and 1573 °C, and the resulting solids were analyzed using SEM-EDS. Increasing reduction temperatures indicated enhanced metallic formation. The metal produced at 1573 °C smelting process from the 500 °C reduction sample contained 79.30% Fe and 15.59% nickel (Ni), while the 700 °C and 900 °C reduction samples contained 74.62% Fe and 14.88% Ni, and 75.57% Fe and 13.77% Ni, respectively.

1 Introduction

As in 2024, world's nickel reserves are estimated to be more than 130 million tons, which around 55 million tons reserved in Indonesia [1]. According to Directorate General of Mineral and Coal report, 60% of Indonesia's nickel ores deposit are lateritic nickel ore, in which derived into two types of ore: saprolite nickel ore with its Ni content varying of 1.5 – 3.0%, and limonite nickel ore with its Ni content varying of 0.8 – 1.5%. Around 70% industrial applications of saprolite ore are in the field of stainless steel production, in which constant market growth over the past year, as reported by Ministry of Energy and Mineral Resources. The conventional route for ferronickel production is the Rotary Kiln-Electric Furnace (RKEF) process, in which nickel ores undergo high-temperature reduction and smelting [2]. In RKEF process, coal-based reductants, such as anthracite coal and coke, are predominantly used during the reduction stage [3]. As a result of the intensive thermal energy requirements and reliance on fossil-based reductants, ferronickel production processes are relatively energy intensive, which their production processes emit 45 – 51 tons of CO₂ to produce 1 ton of ferronickel [4]. The continued use of

coal as a reductant in this process risks escalating carbon emissions in line with growing demand, posing a serious challenge to Indonesia's 2060 Net Zero Emissions target.

In response to these environmental concerns, palm kernel shell (PKS) has attracted growing interest as a renewable and more sustainable reducing agent alternative. In Indonesia, PKS is abundantly available as a waste product from the palm oil industry, with an annual potential reaching approximately 12.8 million tons, as reported by the Directorate General of New, Renewable Energy, and Energy Conservation (EBTKE) in 2022. In addition to its wide availability, PKS is regarded as a carbon-neutral material due to the balance between CO₂ emissions during utilization and CO₂ uptake during the growth of oil palm trees. Its partial substitution for fossil-based reductants can thus contribute to a reduction in overall greenhouse gas emissions, enhancing the environmental sustainability of the process [5]. However, in its raw form, PKS still presents limitations such as low fixed carbon content, high moisture, and high volatile matter, which limit its direct use in high-temperature reduction processes. These unfavorable properties negatively affect its

* Corresponding author: winnywulandari@itb.ac.id

reactivity, stability, and efficiency as a metallurgical reductant.

To improve the performance of PKS, torrefaction (a mild pyrolysis process conducted at 200 – 300 °C under inert atmosphere) has been widely proposed. This thermal pretreatment effectively increases the fixed carbon content, reduces moisture and volatiles, and enhances the overall thermochemical stability of biomass, making torrefied PKS more suitable for high-temperature applications such as lateritic nickel ore reduction [6]. Several studies have demonstrated that torrefied PKS exhibits comparable or even superior reduction capability relative to conventional reductants. For example, Sugiarto et al. [7] reported that using PKS charcoal could achieve nickel recovery levels like those obtained with coke or anthracite. Increasing the dosage of PKS as a reductant not only enhances the mass loss during the reduction process, indicating the release of oxygen from metal oxides, but also promotes the formation of reduced phases such as NiO and FeO in the final product, suggesting a more effective reduction overall [8]. Furthermore, studies by Suharno et al. [9] revealed that higher reduction temperatures significantly improve nickel grade and recovery in the product, supporting the importance of optimizing process conditions.

Building upon these findings, this study aims to further explore the use of torrefied palm kernel shell (PKS) as a reductant in the production of ferronickel from saprolite nickel ore under various operational conditions. The investigation begins by evaluating the impact of the torrefaction process on the fixed carbon content of PKS to understand its enhancement as a thermal pretreatment method. Subsequently, the effects of reduction temperature and holding time are examined in relation to mass loss during the reduction process and the formation of metal oxide phases, which serve as indicators of the extent of reduction. The study also investigates how reduction temperature influences the elemental composition of the reduced metal, as well as the distribution of elements between the metal and slag phases after the melting process. Through this comprehensive evaluation, the research seeks to generate a deeper understanding of the thermochemical behavior of torrefied PKS and its potential as a sustainable and effective alternative to conventional carbon-based reductants in ferronickel production.

2 Experimental

2.1 Raw materials

There are two main raw materials that are used in this study, which are saprolite ore and palm kernel shell. The saprolite ore used in this study was obtained from Sulawesi, Indonesia. Meanwhile, the palm kernel shell was obtained from Sumedang, West Java, Indonesia.

The oxide content within the dried saprolite ore was analyzed using X-ray Fluorescence (XRF, IK.I.3-02, Rigaku Smart Lab), and the result is shown in Table 1. The analysis results confirm that the ore used is indeed saprolite-type ore with 2.79 wt% of NiO, 15.10 wt% of

Fe₂O₃, and high MgO and SiO₂ contents. The minerals present within the dried saprolite ore were also analyzed using X-ray diffraction (XRD, ASTM E3294- 22). The XRD analysis results in Fig. 1 indicate that the saprolite ore used in this study contains serpentine (Mg_{1-x}-y,Fe_x,Ni_y)₃Si₂O₅(OH)₄, quartz SiO₂, goethite FeO(OH), and hematite Fe₂O₃. While most of the iron is contained in goethite and hematite minerals, nickel is mostly embedded in the serpentine crystal [10].

Table 1. Dried saprolite nickel ore composition characterized using XRF

Component	Content (%wt)
MgO	21.40
Al ₂ O ₃	2.03
SiO ₂	55.70
CaO	1.89
Cr ₂ O ₃	0.87
Fe ₂ O ₃	15.10
NiO	2.79
Other constituent*	0.23

*other constituent consist of SO₃, Cl, K₂O, CuO

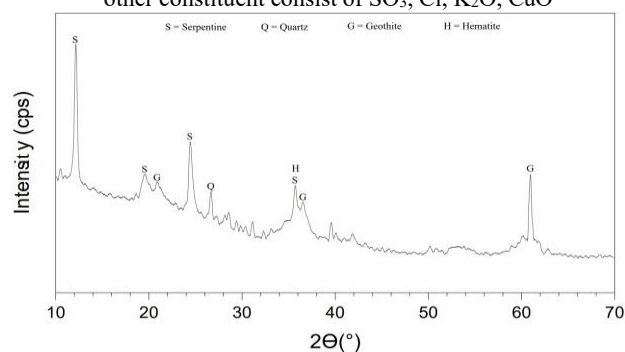


Fig. 1. Dried saprolite nickel ore's crystalline phases obtained from XRD

Meanwhile, the content within the palm kernel shell was analyzed using proximate analysis. The proximate analysis results in Table 2 indicate that the palm kernel shell contains 17.43 wt% of fixed carbon and high volatile matter contents, with a low ash content. Compared to conventional reductant used in industry, typically metallurgical coke contains >85 wt% of fixed carbon, while anthracite coal contains >86 wt% of fixed carbon [11].

Table 2. Proximate analysis of palm kernel shell

Parameters	Content (wt%)
Moisture	10.96
Volatile Matter	70.13
Fixed Carbon	17.43
Ash	1.48

2.2 Preparation of the raw material

Initially, the saprolite nickel ore was crushed using ball mill and then sieved using a vibrating sieve shaker. Later, the crushed saprolite nickel ore with a particle size of -60 +100 mesh were dried in an oven at 105 °C for 2 hours. This fine nickel ore was then utilized for subsequent experiments, with part of it being reserved for characterization via XRF and XRD that the results have been shown in Table 1 and Fig. 1.

Meanwhile, the palm kernel shell was ground using blender. Later, the fine palm kernel was torrefied and utilized for subsequent experiments. However, part of fine palm kernel shell was also reserved for proximate analysis which the results have been shown in Table 2.

2.3 Torrefaction of palm kernel shell

The torrefaction experiments of palm kernel shell were conducted in a vertical tube furnace. The vertical tube furnace was equipped with a calibrated thermocouple to monitor the temperature of furnace's hot zone. This experiment was carried out at 300 °C for 1 hour in the presence of N₂. Flow rate of N₂ gas was maintained at 1 lpm using flow meter to ensure inert condition during torrefaction. The gas output was directed to laboratory's exhaust fan.

Each experiment conducted used 50 grams of palm kernel shell as initial samples, which the results were later mixed. To ensure homogenous samples, the torrefaction product was crushed using ball mill, which then sieved using a vibrating sieve shaker. Later, torrefaction product with a particle size of -60 +100 mesh were torrefied and utilized for subsequent experiments. Part of fine palm kernel shell was also reserved for proximate analysis.

2.4 Reduction of saprolite nickel ore using torrefied palm kernel shell

The reduction experiments of saprolite nickel ore using torrefied palm kernel shell were conducted using a horizontal tube furnace, simulating the rotary kiln processes. The horizontal tube furnace was fitted to ensure gas-tight system and prevent any gas leakage. The gas output was directed to a silicone oil as gas trapper before went into the laboratory's exhaust system. Flow rate of Ar gas was maintained at 1 lpm using flow meter to ensure inert condition during reduction.

The experiments were conducted at varying temperature of 500 °C, 700 °C, and 900 °C, and varying reaction time of 60, 90, and 120 minutes. For each experiment, 15 grams mixture of saprolite nickel ore and torrefied biomass (mass ratio of 4:1) was placed on an alumina boat crucible. Then, the alumina boat crucible that containing reduction sample was placed in the furnace's hot zone at room temperature. The furnace's temperature then raised to target temperature with a rate of 10 °C per minute. After the reduction processes carried out at desired temperature and reaction time, the sample was cooled to room temperature inside the furnace. Each solid reduction was then collected, and its weight was measured to gain insight into the overall reduction processes. Products of reduction process with time reaction of 120 minutes were then used in the subsequent melting process, while part of them were also subjected to characterization to obtain information regarding their bulk composition and present phases.

2.5 Melting of solid reduction product

The solid reduction product obtained from the 120 minutes reduction experiments were melted in a vertical tube furnace, simulating the electric furnace processes. The vertical tube furnace was fitted to ensure gas-tight system and prevent any gas leakage. The gas output was directed to gas trapper before went into the laboratory's exhaust system. Like reduction processes, a flow of Ar gas was maintained at 1 lpm using flow meter to ensure inert condition during reduction.

Approximately 2 grams of solid reduction product was placed in magnesia crucible for each experiment. The sample inside magnesia crucible later introduced inside the furnace and initially positioned at the bottom of the furnace, hung by molybdenum wire. The lower part of the furnace later immersed in water, preventing any inflow of outside's air. After the furnace's inside completely contained Ar gas, inert atmosphere, the sample was then raised into the hot zone that already reached temperature of 1573 °C. The sample was then held at 1573 °C for 120 minutes, which then the sample was quenched by rapidly lowering sample in the crucible into the water at the bottom of the furnace.

The quenched samples later dried by utilizing hot air from hair dryer for approximately 30 minutes. Later, the dried quenched samples were mounted in resin and then were cross sectioned using ceramic cutter at high speed. The cross-sectioned samples were also mounted in resin and their surfaces were polished later. The polished samples were then subjected to characterization.

2.6 Product characterization

The solid reduction products obtained from reduction processes with reaction time of 90 and 120 minutes were analyzed using XRD (ASTM E3294-22). The solid reduction products obtained from reduction processes with reaction time of 120 minutes were also analyzed using scanning electron microscope-energy dispersive x-ray spectroscopy (SEM-EDS, JCM-7000 NeoScope™). Meanwhile, the products of melting processes were analyzed only using SEM-EDS.

3 Results and discussion

3.1 Composition of torrefied palm kernel shell

Following torrefaction at 300 °C, the proximate composition of palm kernel shell (PKS) exhibited significant transformation, as presented in Fig. 2. Both moisture and volatile matter contents decreased substantially due to the evaporation of water and the thermal decomposition of organic constituents, particularly hemicellulose. In contrast, the fixed carbon content increased, attributed to the relative loss of volatiles and the formation of more thermally stable carbonaceous structures. This enhancement in fixed carbon indicates improved reductive potential of the torrefied biomass. The ash content appeared to increase proportionally, not due to the formation of additional ash, but because of overall mass reduction.

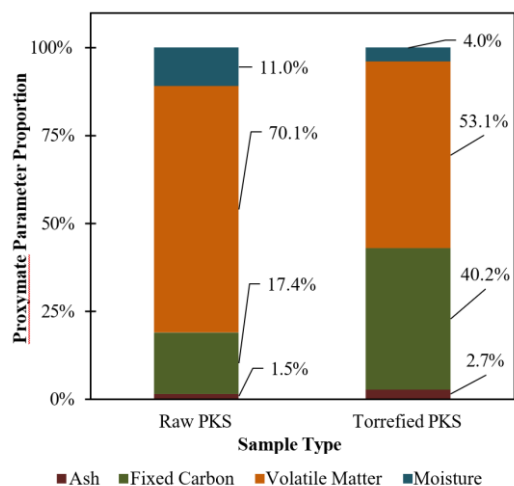


Fig. 2. Proximate parameters of raw and torrefied PKS samples

Table 3. Change in absolute mass of proximate components of PKS due to torrefaction (Basis sample 50 grams)

Parameters	Raw PKS		Torrefied PKS		Change in mass	
	Percent adb (%)	Initial mass (g)	Percent adb (%)	Final mass (g)	Change in mass (g)	Change in mass (%)
Moisture	10.96	5.48	3.98	1.09	-4.39	-80.13
Volatile matter	70.13	35.07	53.12	14.53	-20.53	-58.55
Fixed carbon	17.43	8.72	40.16	10.99	2.27	26.08
Ash	1.48	0.74	2.74	0.75	0.01	1.31
Total mass	100.00	50.00	100.00	27.36	-22.64	-45.28

As shown in Table 3, the torrefaction process resulted in an average mass loss of 22.64 grams, equivalent to 45.28% of the initial 50 g sample. This loss primarily originated from the degradation of volatile matter (-20.53 g, -58.55%) and moisture (-4.39 g, -8.78%), which were released during thermal treatment. On the other hand, fixed carbon increased by 2.27 grams (+26.08%), indicating an accumulation of non-volatile carbon in the solid residue (char), which enhances the PKS's potential as a reducing agent in lateritic nickel ore processing. The slight increase in ash mass (only +0.01 g, +1.31%) further confirms that the increase in ash percentage was solely due to the relative decrease in volatile and moisture components, not from the generation of new inorganic compounds.

3.2 Crystalline phases in the solid reduction products

The crystalline phases formed in the solid products after 90 and 120 minutes of reduction experiments were analyzed using X-ray diffraction (XRD), with the results summarized in Fig. 3. Apart from the crystalline phases present in the initial ore such as serpentine, goethite, hematite, and quartz, several new crystalline phases were detected in the solid reduction products such as olivine, pyroxene, ferronickel, and iron. The appearance of these phases indicates that crystalline transformations occurred during the reduction process.

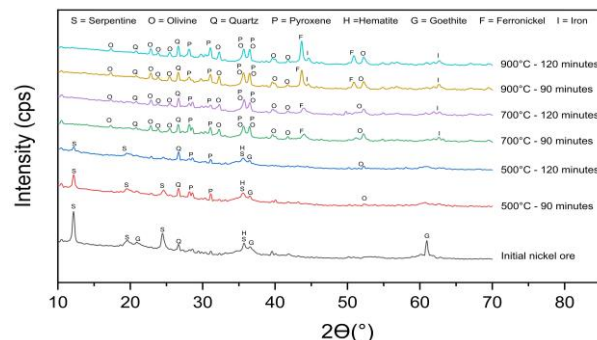
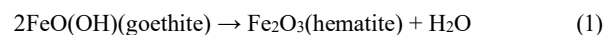
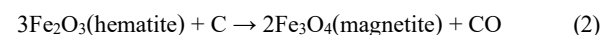


Fig. 3. The effect of temperature and reduction time of saprolite nickel ore using torrefied PKS reductant on the formation of metal oxides based on XRD analysis

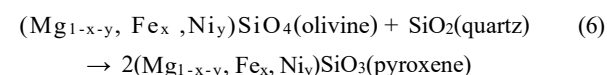
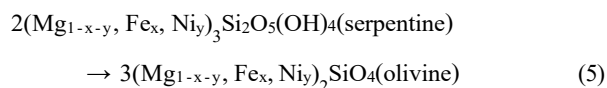
At a temperature of 500 °C, goethite undergoes dehydration to form hematite. The reaction representing this dehydration process can be written as follows [12]:



At a temperature of 700 °C, the hematite phase is no longer detected in the XRD results, indicating that it has undergone complete phase transformation. Under a reducing atmosphere, hematite is gradually reduced through a series of steps, starting with the formation of magnetite (Fe_3O_4), followed by wüstite (FeO), and ultimately reduced to metallic iron (Fe). The reactions representing these transformations are as follows [13]:



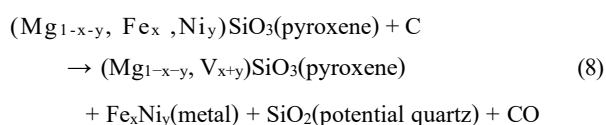
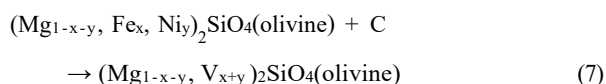
At 700 °C, serpentine is no longer detected in the XRD results, indicating that it has undergone complete thermal decomposition. According to Satritama et al. [10], this process primarily produces olivine as the dominant phase. This transformation pathway was previously proposed by Brindley and Hayami [14], and later confirmed experimentally by Chen et al. [15], who demonstrated that serpentine decomposes into magnesium silicates such as olivine at temperatures exceeding 600 °C. Furthermore, the olivine formed may subsequently react with residual quartz in the system, resulting in the formation of pyroxene. These solid-state phase transformations can be represented by the following reactions [14], [15]:



XRD diffraction peaks of iron and ferronickel metals began to be observed significantly at temperatures of 700 °C, indicating the onset of metallic phase formation within the system. The intensity of these peaks increases progressively with both temperature and reduction time, reflecting the growth of metal crystals and the increasing

yield of reduced metals. The iron-rich metallic phase, confirmed through combined XRD and SEM-EDS analysis, is associated with the stepwise reduction of hematite, as described in Reactions (2) through (4).

Meanwhile, the ferronickel phase, detectable only via XRD, is believed to originate from the gradual reduction of serpentine decomposition products, namely olivine and pyroxene. Thus, the formation pathway of ferronickel can be traced through the reductive transformation of these silicate minerals, and may be simply represented by the following reactions [10], [13]:



In this case, V refers to the metal cation vacancy in the crystal structure of olivine or pyroxene, which can form due to high temperature conditions.

Longer reduction time generally enhances the conversion of serpentine, goethite, and hematite into metallic phases by allowing prolonged interaction between carbon and metal oxides. While the reaction rate slows as readily reducible oxides are consumed, this effect is most pronounced at lower temperatures. As shown in Fig. 3, time-dependent conversion is evident at 500 °C, marked by the shortened serpentine peak. In contrast, at 700 °C and 900 °C, peak changes are minimal, indicating that near-complete conversion is achieved more rapidly.

3.3 Microstructure and phases identification of the solid reduction products

The solid reduction products of 120 minutes reduction processes were further characterized using SEM-EDS to identify their microstructures and its phases composition. These samples were mounted in resin and polished before analyzed. Fig. 4 shown an example backscattered image obtained, which was solid reduction product of 900 °C reduction process. In general, solid reduction product consisted of 3 phases, in which the white area was phase rich of Fe contents, while the light-grey and dark-grey area indicates olivine and pyroxene phases.

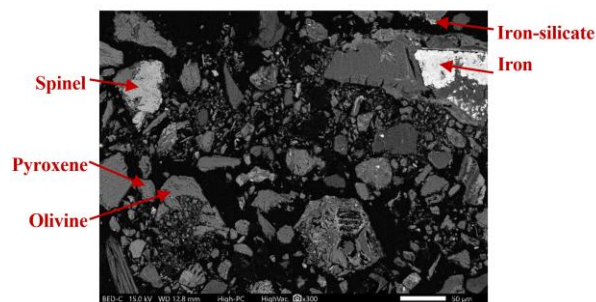


Fig. 4. SEM backscattered image of the solid reduction product at 900 °C for 120 minutes

Table 4. Average phase compositions of solid reduction product

120 minutes reduction		Composition (%w/w)							
T _{Reduction} (°C)	Phase	M	Fe	Ni	Cr	Si	Mg	Al	Ca
		O	FeO	NiO	Cr ₂ O ₃	SiO ₂	MgO	Al ₂ O ₃	CaO
500	Iron-silicate	O	91.17	0.71	0.16	4.25	3.58	0.09	0.03
	Pyroxene	O	5.67	2.96	0.27	51.57	37.76	1.62	0.16
	Pyroxene	O	14.16	4.03	-	53.54	27.11	0.99	0.17
	Olivine-Ni	O	12.07	40.70	0.38	24.84	16.39	5.32	0.30
700	Iron	M	96.17	0.05	0.09	0.75	0.29	0.05	0.12
	Iron-silicate	O	32.47	2.18	0.37	55.50	7.52	1.56	0.40
	Olivine	O	3.56	0.36	2.76	37.30	37.11	18.26	0.65
	Pyroxene	O	13.13	3.56	0.16	47.51	34.84	0.67	0.13
900	Iron	M	95.67	0.28	0.17	2.09	1.47	0.03	0.30
	Iron-silicate	O	12.60	0.60	0.42	85.74	0.43	0.15	0.06
	Olivine	O	11.93	0.76	0.06	42.17	44.84	0.11	0.13
	Pyroxene	O	2.64	0.25	1.11	55.11	22.76	6.69	11.44
	Spinel	O	23.31	0.38	38.43	0.61	10.22	26.89	0.06

*Metallic phases are labeled as M, while oxide phases are labeled as O

The average phase compositions of each sample are shown in Table 4. It was found that at 500 °C reduction, its rich-Fe contents were not in metallic phase, but is an iron-silicate. These findings confirm that at 500 °C reduction process there was no metals were formed, similar to previous XRD results. However, solid reduction products from reduction at 700 °C and 900 °C were also indicated iron-silicate phases, although with lower Fe content compared to the 500 °C reduction sample. This is attributed to the fact that most of the Fe had already formed metallic iron phases upon reduction, leaving only a small amount of Fe oxides present in the iron-silicate, pyroxene, or olivine phases. Additionally, in the 500 °C reduction sample, a Ni-rich olivine phase was identified, containing up to 40.70% NiO. In the 900 °C reduction sample, a spinel phase was also detected, consisting of Cr₂O₃, FeO, and Al₂O₃.

3.4 Overall reduction extent of nickel saprolite ore reduction using torrefied palm kernel shell

The effect of reduction temperature and holding time on mass loss is presented in Fig. 5. In general, the graph shows that mass loss increases with both higher temperatures and longer reduction durations. This trend suggests that as the thermal energy increases, more components within the nickel ore and torrefied PKS mixture undergo decomposition or reduction reactions. Although the overall trend is upward, the increase in mass loss with longer reduction time is not always linear. At 700 °C, for example, the mass loss observed at 1.5 hours was slightly higher than at 2 hours, which may be attributed to minor experimental variability. More importantly, at 900 °C, the mass loss remained relatively constant in the range of 21.4 – 22.0% across all holding times, indicating that the system had likely reached equilibrium. This implies that higher temperatures enable the system to attain equilibrium more rapidly, thus requiring less time for the reactions to complete. Consequently, extending the reduction duration beyond this point yields minimal additional effects. Temperature, therefore, plays the dominant role

in driving the reduction process, while holding time serves mainly to facilitate reaction completeness, particularly at lower temperatures.

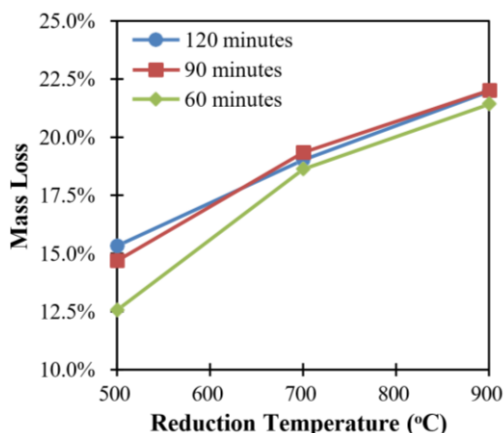


Fig. 5. Reduction sample’s mass loss in relation to reduction temperatures and times

In addition to the reduction of metal oxides in the nickel ore, mass loss also results from the thermal decomposition of residual volatile compounds in the torrefied PKS. Despite undergoing torrefaction, the reductant still contains trace organic volatiles that may decompose at elevated temperatures, particularly above 700 °C. Therefore, the observed mass loss reflects both physical and chemical transformations within the ore–reductant mixture.

3.5 Microstructure and phases identification of the melting products

As stated previously, samples of solid reduction products were melted in vertical tube furnace to simulate processes occurred in electric furnace. Fig. 6 shown an example of backscattered image of the melting product from the solid reduction products obtained from 900 °C reduction process. The melting product phases are metal, slag, and pyroxene. The metallic phase was observed as a large white droplet and little droplets scattered around the slag phase that was observed as light-grey surface around the metal. Within the slag, the pyroxene phase existed and observed as dark-grey surface.

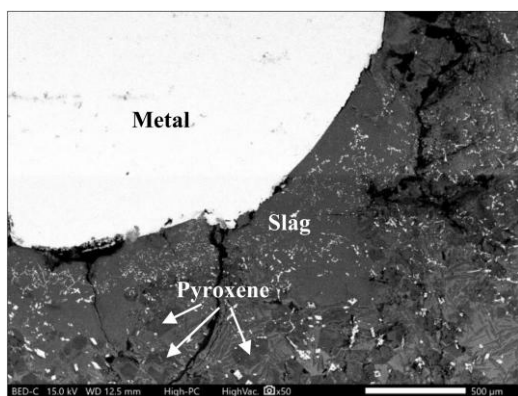


Fig. 6. SEM backscattered image of the smelted sample from the solid reduction product at 900 °C for 120 minutes after smelting at 1573 °C for 120 minutes

3.6 Compositions of the melting products

Average compositions of each phase in melting products were semi-quantitatively measured using SEM-EDS, which compiled in Table 5. The measurement shows that the slag and pyroxene were contained very low Fe (< 2 wt %). While in previous analysis of solid reduction product at 500 °C reduction process was not shown any metal phases, a metal phase consisting of 79.30 wt% Fe and 15.59 wt% Ni were formed. Thus, indicates that the smelting process led to re-equilibration and metals combined.

Table 5. Average phase compositions of smelted solid reduction products

1573°C Smelting		Composition (%w/w)							
T _{Reduction} (°C)	Phase	M	Fe	Ni	Cr	Si	Mg	Al	Ca
		O	FeO	NiO	Cr ₂ O ₃	SiO ₂	MgO	Al ₂ O ₃	CaO
500	Metal	M	79.30	15.59	1.68	2.13	0.19	0.05	0.07
	Slag	O	1.04	0.03	0.94	58.53	33.39	2.55	3.51
	Pyroxene	O	0.67	0.02	0.24	43.68	54.94	0.31	0.13
700	Metal	M	74.62	14.88	2.44	6.37	0.12	-	0.01
	Slag	O	0.52	0.05	0.56	62.94	31.85	2.34	1.74
900	Metal	M	75.57	13.77	2.19	6.10	0.30	0.02	0.11
	Slag	O	1.24	0.11	1.11	63.16	29.71	2.33	2.33
	Pyroxene	O	1.58	0.39	0.19	43.69	53.21	0.33	0.62

*Metallic phases are labeled as M, while oxide phases are labeled as O

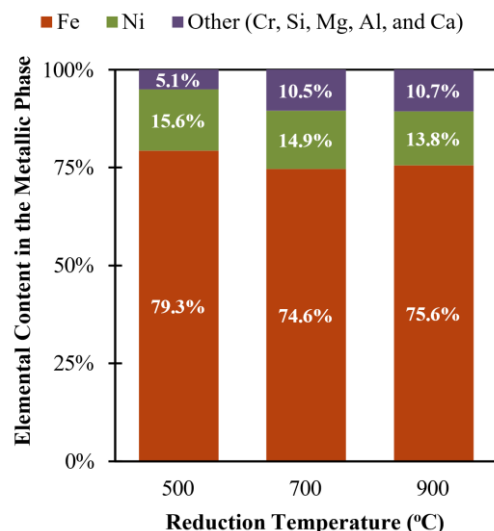


Fig. 7. Elemental content of the metallic phases in the smelting products.

Fig. 7 shows the elemental content of the metallic phases in the smelting products, which is dominated by Fe and Ni. In general, higher reduction temperature led to Ni contents decreasing in terms of mass percentage. However, due to the metal phases enlargement as reduction temperature increased, the amount of Ni contents in metal produced were increased. The decline of Ni mass percentage in metal produced as reduction temperature increased were caused by more-significant Fe contents increased. Although, metal sample from

500 °C reduction process was found to be had the highest Fe content (79.30 wt%). It was also found that those sample had the lowest contents of Cr and Si, thus increasing its Fe content due to low contents of residue. While higher reduction temperatures generally facilitate metal oxide reduction, the results in this study do not show a consistent trend with temperature, as fluctuations in FeO content were observed, particularly in the slag and pyroxene phases. These fluctuations may be attributed to multiple interacting factors, highlighting the complexity of the reduction process.

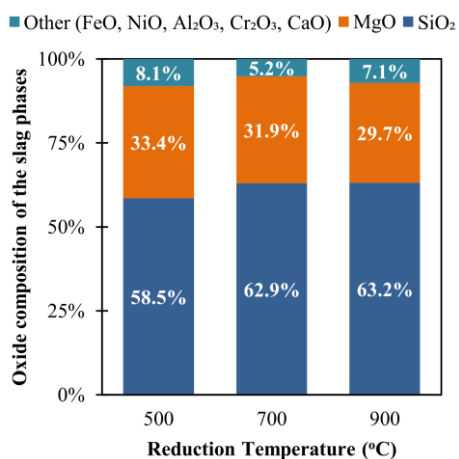


Fig. 8. Oxide composition of the slag phases.

The slag compositions from all samples are also plotted in Fig. 8. In general, higher reduction temperature led to SiO₂ increasing contents in slag phase, while the MgO contents were decreased. However, the change of slag contents was not as significant as metal content.

The present findings suggest that torrefied biomass, specifically palm kernel shell, is feasible and holds potential for ferronickel production processes. Therefore, the usage of coke as reductant could be replaced by torrefied palm kernel shell in the effort of achieving Net Zero Energy. However, it is important to note that the environmental friendliness of biomass usage is dependent on the production method.

4 Conclusion

This study investigated experimental reduction of saprolite nickel ore using torrefied palm kernel shell as reductant, with a variation of temperature and reduction time. Torrefied palm kernel shell indicated an increase in fixed carbon content for 22.64%. A series of experiments were carried out to simulate the process occurring in rotary kiln and electric arc furnace. Reduction of saprolite nickel ore using torrefied palm kernel shell were carried out in horizontal tube furnace at Ar atmosphere, with variate conditions of temperature 500 °C, 700 °C, and 900 °C, and reaction times of 60, 90, and 120 minutes. It was found that increased temperature led to increase in metallic phase formation, while increased reaction time did not significantly influence the results. Same results were also shown in terms of mass loss, in which the equilibrium condition is tend to temperature dependent. Several phases that

were identified in the solid reduction products were iron-silicate, pyroxene, olivine, iron, and ferronickel. The solid reduction products obtained were later smelted in vertical tube furnace at 1573 °C for 120 minutes under Ar atmosphere. The smelting processes resulted in metal and slag formation, with pyroxene remained. It indicates increased reduction temperature led to decreased in metal's Ni content, which at 500 °C resulted in Ni 15.59 wt pct, at 700 °C resulted in Ni 14.88 wt pct, and at 900 °C resulted in Ni 13.77 wt pct. It is also shown that highest metal's Fe content was at 500 °C reduction temperature, approximately 79.30 wt pct. However, the slags composition were not significantly affected by reduction temperatures. In general, metals composition produced in these studies are within the range of the commercially produced nickel pig iron.

This research is funded through Program Penelitian, Pengabdian Masyarakat, dan Inovasi ITB (PPMI ITB) with the contract no. FTI-PPMI-1-31-2023.

References

- USGS, Mineral commodity summaries 2025, (2025). <https://doi.org/10.3133/mcs2025>
- F. K. Crundwell, M. S. Moats, V. Ramachandran, T. G. Robinson, and W. G. Davenport, Overview of the Smelting of Nickel Laterite to Ferronickel, Extractive Metallurgy of Nickel, Cobalt and Platinum Group Metals, 49–53 (2011). <https://doi.org/10.1016/B978-0-08-096809-4.10004-8>
- G. Hang, Z. Xue, and Y. Wu, Preparation of high-grade ferronickel from low-grade nickel laterite by self-reduction and selective oxidation with CO₂-CO gas, Miner. Eng. **151**, (2020). <https://doi.org/10.1016/j.mineng.2020.106318>
- Nickel Institute, Life cycle data 2025, (2025)
- B. C. Pamungkas and H. Hadi, Potential of Biomass Utilization in Rotary Kiln of Nickel Processing Plant, IOP Conf. Ser. Mater. Sci. Eng. **588**, (2019). <https://iopscience.iop.org/article/10.1088/1757-899X/588/1/012006>
- H. F. Qinthara, N. M. D. S. Anggraeni, W. Wulandari, D. Sasongko, and T. Hidayat, Torefaksi Biomassa Untuk Campuran Batubara sebagai Reduktor Peleburan Bijih Nikel Saprolit, Bachelor Thesis, Institut Teknologi Bandung, (2023)
- E. Sugiarto, A. D. P. Putera, and H. T. B. M. Petrus, Kinetic study of nickel laterite reduction roasting by palm kernel shell charcoal, IOP Conf. Ser. Earth Env. Sci. **65**, (2017). <https://iopscience.iop.org/article/10.1088/1755-1315/65/1/012027>
- B. Satritama, Z. Zulhan, T. Hidayat, and N. Halim, Substitusi Batubara dengan Gas Hidrogen

- atau Biomassa Cangkang Kelapa Sawit pada Peleburan Bijih Nikel Saprolit untuk Produksi Paduan Feronikel, Bachelor Thesis, Institut Teknologi Bandung, (2023)
9. B. Suharno, N. P. Iman, A. Shofi, D. Ferdian, and F. Nurjaman, Study of Low-Grade Nickel Laterite Processing Using Palm Shell Charcoal as Reductant, *Mat. Sci. For.* **1000**, 436–446 (2020).
<https://doi.org/10.4028/www.scientific.net/MSF.1000.436>
 10. B. Satritama, Z. Zulhan, W. Wulandari, D. Sasongko, A. Y. Al Hakim, and T. Hidayat, The Impacts of Temperature, Gas Composition and Reaction Time on the Reduction of Saprolite Nickel Ore Under Hydrogen–Argon Atmosphere, *Metal. and Mat. Tran. B: Proc. Metal. and Mat. Proc. Sci.* **55**, 396–408 (2024).
<https://doi.org/10.1007/s11663-023-02965-4>
 11. P. Grammelis, N. Margaritis, and E. Karampinis, Solid fuel types for energy generation, *Fuel Flex. Ene. Gen.*, 29–58 (2016).
<https://doi.org/10.1016/B978-1-78242-378-2.00002-X>
 12. Sufriadin, D. Adrianus, M. Z. Mubarak, A. Saputno, and A. Ito, Mineralogical transformation and Ni enrichment through reduction roasting of limonite ore from the Tinanggea area, South Konawe, Southeast Sulawesi, *IOP Conf. Ser. Earth Env. Sci.* **1517**, (2025).
<https://iopscience.iop.org/article/10.1088/1755-1315/1517/1/012034>
 13. A. J. Nabilah, B. Satritama, T. Hidayat, P. Taskinen, I. Santoso, H. Kurniadani, and Z. Zulhan, Reduction of saprolite nickel ore using methane-argon gas mixture with laboratory-scale simulated rotary kiln-electric furnace (RKEF) technology, *Miner. Eng.* **234**, (2025).
<https://doi.org/10.1016/j.mineng.2025.109776>
 14. G. W. Brindley and R. Hayami, Mechanism of formation of forsterite and enstatite from serpentine, *Miner. Mag. and J. of the Miner. Soc.* **35**, 189–195 (1965).
<https://doi.org/10.1180/minmag.1965.035.269.21>
 15. J. Chen, E. Jak, and P. C. Hayes, Factors influencing the microstructures of iron ore sinters, *Miner. Proc. and Ext. Metal.* **130**, 181–191 (2021),
<https://doi.org/10.1080/25726641.2019.1684712>